Spasmodic growth during the rapid solidification of undercooled Ag-Cu eutectic melts

C. R. Clopet, R. F. Cochrane, and A. M. Mullis
Institute for Materials Research, University of Leeds, Leeds LS2 9JT, United Kingdom

(Received 5 August 2012; accepted 21 December 2012; published online 23 January 2013)

A melt fluxing technique has been used to undercool Ag-Cu eutectic alloy by 10–70 K and the subsequent recalescence has been studied using high speed imaging. Spasmodic growth of the solidification front was observed, in which the growth front would make a series of quasi-periodic jumps separated by extended periods during which time growth appeared to arrest. Evidence of this previously unreported mode of growth is presented. The high speed images and microstructural evidence support the theory that anomalous eutectics form by the growth and subsequent remelting of eutectic dendrites. © *2013 American Institute of Physics*. [http://dx.doi.org/10.1063/1.4775670]

With increasing departures from equilibrium, a number of morphological changes are observed during the growth of eutectic alloys. In particular, as the liquid is progressively undercooled a number of systems, including Ni-Sn,[1–6] Ni-Si,[7–9] Co-Sb,[7] Co-Sn,[8,10,11] Co-Al,[9] Co-Mo,[12] Co-Si,[13] and Ag-Cu,[14–19] have been reported to display a transition from a regular lamellar to an anomalous eutectic structure. In most cases, this is a progressive transition, with increasing volume fractions of the anomalous eutectic being formed as the undercooling is increased. For such materials with a mixed lamellar/anomalous eutectic structure, such as Ag-Cu at low undercooling, it has been suggested that the anomalous structure is a direct product of rapid solidification, forming first, with the eutectic lamellae growing slowly after the initial recalescence event.[15]

The anomalous structure occurring in undercooled eutectic Ag-Cu alloy has been found to grow in "zones" in the direction of solidification.[16,19] At low undercoolings, Zhao *et al*. observed two or three zones which developed in concentric bands from the nucleation point. In the first zone, a purely anomalous structure was formed, however, further from the nucleation point, there was a shift to a cellular structure that took the form of columnar, then equiaxed, grains or just columnar grains depending on level of undercooling. These grains consisted of lamellar eutectic with anomalous eutectic at the grain boundaries. It was inferred from these evolved microstructures that non-steady state solidification occurred and the growth velocity gradually decreased across the samples. However, the progression of the growth front across the sample was not recorded and direct measurements of the growth velocity were not made.

There has been much debate on the formation mechanism of anomalous eutectics. Suggestions for the mechanism have included the decomposition of a dendritic supersaturated single-phase solid-solution,[2] decoupled growth of the lamellar eutectic,[3,8,12,20] fragmentation or remelting of primary lamellar eutectics,[5,7,11,16,19] and remelting of eutectic dendrites.[17,18] The issue has been clarified somewhat by the recent work of Yang *et al*.[6] who observed that, within the same alloy, the anomalous eutectic may have a dual origin. At relatively low undercoolings (~40 K), a fine grained anomalous eutectic was formed which they concluded was due to the remelting of eutectic dendrites, while at high undercooling (~202 K), a coarse grained anomalous eutectic was formed by partial remelting of single phase dendrites. However, there are relatively few systems in which eutectic growth is reported to occur at such high undercoolings. Li and Zhou[21] suggested that such growth is probably restricted to systems in which at least one of the solidifying phases is an intermetallic, which would be the case for Ni-Sn, where the eutectic is formed between α-Ni and Ni_3Sn intermetallic. Consequently, the most likely origin for anomalous eutectic formation at low undercoolings, and certainly in alloys in which both eutectic phases are solid solutions, would seem to be partial remelting of eutectic dendrites.

In single phase alloys, instability of a planar growth front can occur as a solute-rich boundary layer builds up in front of the interface. This leads to perturbations of the interface that do not melt back as the temperature of the liquid ahead of the interface is below the liquidus temperature, causing the formation of cells or dendrites. In contrast, in a pure binary eutectic, a planar growth front is stable against the growth of such perturbations. However, the presence of a third, or impurity, element can destabilize the front as the tertiary solute can accumulate ahead of the growth front, leading to eutectic cells or dendrites. Similarly, in an undercooled eutectic melt, the negative temperature gradient ahead of the growth front can also destabilize it, again giving rise to eutectic cells or dendrites.

In one study of Ag-Cu eutectic alloy,[16] it was suggested that the formation of a cellular structure was possibly due to the large thermal diffusivity of the alloy melt and the large difference in the composition of the two phases, rather than due to the presence of an impurity element. This was further investigated in a study looking at the effect of the inclusion of small amounts of Sb in Ag-Cu alloys.[19] It was found that the addition of a third component caused a transition from cellular to dendritic structure at low undercoolings.

High speed video imaging is a useful technique that may be employed to monitor the progression of the solid-liquid interface during undercooling experiments. This type of imaging has been used to measure the growth velocities for a number of undercooled pure elements and alloys, including pure Si and Ge,[22] Ni-Al,[23] Ni-Ge,[24] Ni-Si,[25] and Ni-Sn[1,3,6] alloys.

In this letter, the results of high speed imaging of fluxing experiments on Ag-Cu eutectic alloy samples are presented. The types of microstructure formed are explained in terms of the new evidence gained from the high speed images, which show that, rather than propagating across the sample in a continuous manner, the progress of the recalescence front is characterized by a series of jumps and pauses, a phenomenon that we describe here as spasmodic growth.

A high purity Ag-Cu ingot of eutectic composition was produced using silver and copper shot, each of 99.9999% purity (metals basis). The metal shot was sealed under argon in quartz tube, heated, and agitated whilst molten to promote mixing before being quenched into water. Small samples of alloy, of approximately 0.8 g, were cut from the ingot and used in the undercooling experiments.

Melt fluxing was selected as a suitable processing technique as undercooled samples can be produced and high speed video capture of solidification is possible with this method. A 10×20 mm fused quartz crucible containing a sample and ground flux was placed on a stand in a stainless steel vacuum chamber, shielded by a graphite susceptor and an alumina shield, within an induction coil. The flux comprised a 50:50 mixture of ground soda lime glass and boron oxide to provide molten glass of the correct viscosity in order to encapsulate the sample in the desired temperature range. The sealed chamber was evacuated to approximately 10^{-3} Pa before being backfilled to 5×10^4 Pa with dried nitrogen gas. The glass flux was dewatered *in situ* and each sample was then subjected to a heating regime using rf induction heating of the susceptor. The temperature of the sample was monitored during the experiment using a k-type thermocouple, which was positioned at the base of the crucible. Full details of the experimental arrangement have been published previously.[26]

A superheat of 250–290 K above the liquidus temperature was imposed on each sample and held for 12 min before allowing the sample to cool to below the melting point. The heating cycle was repeated seven times for each alloy melt. This allowed the molten flux, which isolated the molten sample from the solid crucible, to purify the sample by drawing away any impurities from the metal, further inhibiting nucleation. The samples were then allowed to cool to below the liquidus temperature and nucleate spontaneously. A Photron Fastcam SA5 high speed camera equipped with a Micro Nikkor 70-180 mm zoom lens was used to record the solidification front at frame rates of either 250 or 500 fps.

The fluxed samples were mounted in Bakelite, cut in the plane parallel to the direction of growth, ground using SiC papers, and polished with a series of increasingly fine diamond compounds. All samples were then imaged using a Philips XL30 ESEM.

Eutectic Ag-Cu alloy samples undercooled by 10−70 K, in approximately 10 K steps, were obtained, which exhibited both lamellar and anomalous eutectic microstructures. High speed imaging of the solidification of the undercooled samples meant that the nucleation site could be located in most cases and that the direction, nature and progression of growth front could be followed. Fig. 1 shows the structure of a sample undercooled by 40 K prior to nucleation. The microstructure is cellular, with a typical "cell" consisting of lamellar eutectic in the body of the cells with anomalous eutectic occurring at the cell boundaries. Zones of microstructures were also observed with an initial radial zone of anomalous structure followed by a cellular region of both lamellar and anomalous eutectic. It appears that the development of the anomalous structure from the initial zone into the cellular zone was aligned with the growth direction, as determined by the high speed imaging, and took the form of branched "fingers." These fingers propagated from the initial zone through the entire sample, with the volume fraction of this growth mode gradually reducing in favor of lamellar eutectic growth.

Growth was observed to proceed by means of the propagation of a single, directional front in all cases. However, the progress of the front was spasmodic in that the progress of the interface was not steady, but appeared to start and stop with lengthy time intervals between cessation of the growth front and its continuation. The size of these "jumps" varied over the solidification time, as did the intervening time between jumps. Fig. 2 shows three images taken during the solidification of an Ag-Cu alloy melt undercooled by 40 K, at (a) 1.368 s, (b) 1.584 s, and (c) 1.612 s after nucleation, with the nucleation site and growth direction being indicated in (a). The position of the growth front at $t = 1.368$ s is indicated in (b) and (c), from which it is evident that the front is stationary in the 0.216 s between the capture of the frames shown in (a) and (b) but jumps forward significantly in the 0.028 s between the capture of the frames shown in (b) and (c).

Analysis of the high speed images from the undercooling experiments has been undertaken by measuring the time-dependent average brightness (pixel grey level) along a line projected across the sample from the nucleation point in the direction of growth. The resulting time series has been scaled to 0-1 by subtracting the grey level prior to recalescence and

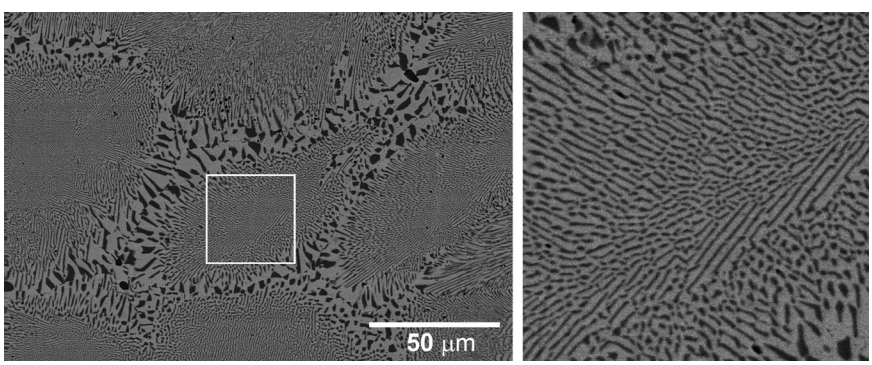

FIG. 1. Micrograph (left) showing the structure of an Ag-Cu alloy undercooled to 40 K prior to solidification. The structure is cellular with regular eutectic in the cell center and anomalous eutectic at the cell boundaries. Magnified region (right) from cell center (delineated by white square).

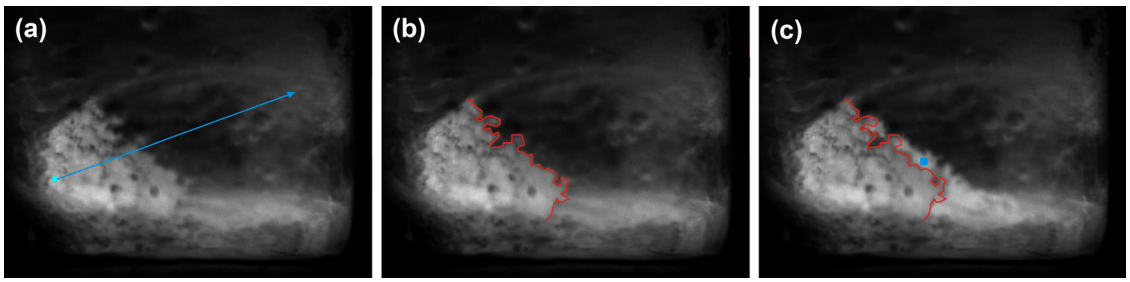

FIG. 2. High speed video images of the solidification interface of an Ag-Cu alloy undercooled by 40 K prior to nucleation. Frames are taken at (a) t = 1.368 s, (b) t = 1.584 s, and (c) t = 1.612 s after nucleation. The nucleation point and growth direction are shown in (a). The boundary line in (b) and (c) denotes the location of the solid-liquid interface at t = 1.368 s (enhanced online) [URL: http://dx.doi.org/10.1063/1.4775670.1].

dividing by the average increase in grey level at the end of recalescence. For a sample recalescing to the melting temperature in which the solid remains isothermal after recalescence, this measure can be used as a proxy for the relative distance the front has travelled along the sample as a function of time, although the data have not been corrected for the viewing geometry and hence show distance in the 2D viewing plane. A composite brightness-time plot for the samples undercooled by 27, 40, and 51 K is shown in Fig. 3. In order to plot all three curves on the same axes, the time is shown relative to a characteristic time, τ_0, for solidification of the sample. The values of τ_0 are 12 s, 5 s, and 4 s for 27 K, 40 K, and 51 K, respectively.

In each case, the first half of the solidification process can clearly be seen to compose of quasi-periodic intervals in which there is little movement of the front, followed by a rapid jump forward in the position of the front. Immediately after a jump forward, the newly formed solid has a maximum brightness. The new solid then appears to cool (decrease in brightness) prior to the next solidification "jump" being initiated. This is seen in Fig. 3 as a decrease in the average brightness between consecutive forward jumps of the solidification front. During this period, the solidification front remains stationary, the decrease in average brightness does not indicate that the solidification front retreats.

The magnitude of this effect has been estimated at one point, indicated by the blue square in Fig. 2(c), a 7 × 7 pixel sample window. Prior to recalescence the grey level inside the sample window was 37 ± 2 (mean ± standard deviation). Immediately following recalescence, the grey level was 152 ± 12, while immediately prior to the next recalescence this had dropped to 116 ± 5.

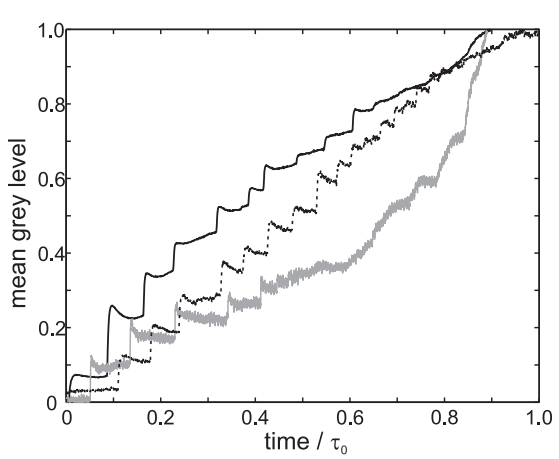

FIG. 3. Plot of the scaled average grey level along a line from the nucleation point and in the growth direction for the recalescence front in an Ag-Cu alloy sample undercooled by 27 K (grey), 40 K (black, solid), and 51 K (black, dashed). The characteristic time, τ_0, is 12 s at 27 K, 5 s at 40 K, and 4 s at 51 K.

In the latter part of the recalescence, the time intervals between jumps become significantly shorter with the progress of the front eventually approaching continuous. This change in propagation characteristics was reflected in the microstructure, as there was an observed shift to an increasingly lamellar structure towards the end of the solidification.

The post recalescence drop in the grey level (cooling) of the solid during spasmodic growth is in contrast to the case where the growth front is observed to propagate in a steady, continuous manner, wherein we observe the brightness after recalescence to be approximately constant. For instance, in the latter stages of solidification of a sample undercooled by 59 K, wherein continuous growth is observed, we measure the grey level at the recalescence front as 108 ± 2, while the grey level at the same location 0.75 s after recalescence was 106 ± 2. Moreover, where both spasmodic and continuous growth is observed in the same sample, the recalescence events during the jumps are brighter than the recalescence during the continuous growth phase. Assuming that during continuous growth recalescence is to the eutectic temperature this would suggest that the recalescence events during spasmodic growth are to a temperature above the equilibrium eutectic temperature. If so, this may account for the remelting that gives rise to anomalous eutectics. However, the non-linearity of the CCD response means that any attempt at estimating either the recalescence temperature or the temperature of the solid after recalescence will be subject to large uncertainties.

From the results of the high speed imaging experiments, it is clear that the spasmodic growth, and hence the formation of the resulting anomalous eutectic, is not due to copious nucleation. In all cases, growth proceeds by the propagation of a front that originates from a single point and we consider that the most likely origin for the anomalous eutectic is the growth, and subsequent remelting, of eutectic dendrites, as suggested by Zhao *et al.*[17,18] The observed spasmodic propagation of the growth front would therefore be related to the growth mechanism of such eutectic dendrites. This type of non-steady behavior is highly unusual in crystal growth and would seem to indicate that the system may not be able to find a single, stable operating point, and is therefore oscillating between two growth modes. In this regard, there may be

parallels with other solidification phenomena, such as the oscillatory two-phase structures found in some peritectic systems.[27]

The basic theory of eutectic growth is described in the classic paper by Jackson and Hunt[28] and subsequently extended to include rapid solidification effects by Trivedi *et al*.[29] and Kurz and Trivedi,[30] although in both cases under the assumption of a positive temperature gradient ahead of the growing eutectic front. A partial model of eutectic growth into undercooled melts has been given by Li and Zhou,[21] although their model suggests, contrary to the observations presented here, that once established eutectic dendrites propagate in a steady-state fashion at uniform velocity. However, as the authors themselves point out, much of the important physics of dendritic growth (e.g., the role of anisotropy) is missing from the model of Li and Zhou and indeed it is far from clear how one could include the anisotropy of a two-phase system into an analytical model of eutectic dendrite growth. Phase-field modeling may in principle be able to offer an explanation for the observed phenomenon, although currently multi-phase models capable of simulating eutectic growth only work in the isothermal limit, wherein the destabilizing negative temperature gradient ahead of the solid-liquid interface is absent, while coupled thermo-solute models are currently only capable of simulating a single solid phase (e.g., Ref. 31).

In summary, anomalous and cellular zones have been observed in undercooled Ag-Cu eutectic melts, with regions of anomalous eutectic structure closest to the nucleation point and a distinct change to a cellular structure as radial distance from the site of nucleation increases. High speed imaging of the undercooled alloy melts monitored the growth of the solidification fronts, from which brightness-time plots were determined. This high speed imaging shows that the growth of the solid-liquid interface is spasmodic, that is, it consists of a series of quasi-periodic jumps, which are separated by extended periods during which time growth appears to arrest. No current models of eutectic growth appear capable of explaining the observed growth mode.

[1]M. Li, K. Nagashio, and K. Kuribayashi, Mater. Sci. Eng., A **375–377**, 528 (2004).
[2]T. Z. Kattamis and M. C. Flemings, Metall. Trans. **1**, 1449 (1970).
[3]M. Li, K. Nagashio, and K. Kuribayashi, Acta Mater. **50**, 3241 (2002).
[4]J. F. Li, W. Q. Jie, S. Zhao, and Y. H. Zhou, Metall. Mater. Trans. A **38**, 1806 (2007).
[5]J. F. Li, X. L. Li, L. Liu, and S. Y. Lu, J. Mater. Res. **23**, 2139 (2008).
[6]C. Yang, J. Gao, Y. K. Zhang, M. Kolbe, and D. M. Herlach, Acta Mater. **59**, 3915 (2011).
[7]R. Goetzinger, M. Barth, and D. M. Herlach, Acta Mater. **46**, 1647 (1998).
[8]M. Li and K. Kuribayashi, Metall. Mater. Trans. A **34**, 2999 (2003).
[9]E. Cadirli, D. M. Herlach, and T. Volkmann, J. Non-Cryst. Solids **356**, 461 (2010).
[10]B. Wei, D. M. Herlach, F. Sommer, and W. Kurz, Mater. Sci. Eng., A **173**, 355 (1993).
[11]L. Liu, J. F. Li, and Y. H. Zhou, Acta Mater. **59**, 5558 (2011).
[12]B. Wei, D. M. Herlach, F. Sommer, and W. Kurz, Mater. Sci. Eng., A **181/182**, 1150 (1994).
[13]W. J. Yao, N. Wang, and B. Wei, Mater. Sci. Eng., A **344**, 10 (2003).
[14]S. Walder and P. L. Ryder, J. Appl. Phys. **73**, 1965 (1993).
[15]N. Wang, C. D. Cao, and B. Wei, Adv. Space Res. **24**, 1257 (1999).
[16]S. Zhao, J. F. Li, L. Liu, and Y. H. Zhou, Mater. Charact. **60**, 519 (2009).
[17]S. Zhao, J. F. Li, L. Liu, and Y. H. Zhou, Chin. Phys. B **18**, 1917 (2009).
[18]S. Zhao, J. F. Li, L. Liu, and Y. H. Zhou, J. Cryst. Growth **311**, 1387 (2009).
[19]S. Zhao, J. F. Li, L. Liu, and Y. H. Zhou, J. Alloys Compd. **478**, 252 (2009).
[20]B. L. Jones, Metall. Trans. **2**, 2950 (1971).
[21]J. F. Li and Y. H. Zhou, Acta Mater. **53**, 2351 (2005).
[22]T. Aoyama and K. Kuribayashi, Mater. Sci. Eng., A **304–306**, 231 (2001).
[23]H. Assadi, S. Reutzel, and D. M. Herlach, Acta Mater. **54**, 2793 (2006).
[24]R. Ahmad, R. F. Cochrane, and A. M. Mullis, J. Mater. Sci. **47**, 2411 (2012).
[25]R. Ahmad, R. F. Cochrane, and A. M. Mullis, Intermetallics **22**, 55 (2012).
[26]S. E. Battersby, R. F. Cochrane, and A. M. Mullis, Mater. Sci. Eng., A **226**, 443 (1997).
[27]M. Vandyoussefi, H. W. Kerr, and W. Kurz, Acta Mater. **48**, 2297 (2000).
[28]K. A. Jackson and J. D. Hunt, Trans. Metall. Soc. AIME **236**, 1129 (1966).
[29]R. Trivedi, P. Mangin, and W. Kurz, Acta Metall. **35**, 971 (1987).
[30]W. Kurz and R. Trivedi, Metall. Trans. A **22**, 3051 (1991).
[31]J. Rosam, P. K. Jimack, and A. M. Mullis, Acta Mater. **56**, 4559 (2008).